JOURNAL OF MATERIALS SCIENCE **34** (1999) 5543–5548

Effect of grain growth and measurement on fracture toughness of silicon nitride ceramics

JIANFENG YANG*, TOHRU SEKINO, KOICHI NIIHARA
The Institute of Scientific and Industrial Research, Osaka University, 8-1 Mihogaoka, Ibaraki, Osaka 567-0047, Japan
E-mail: yangjf@nirin.go.jp

Two kinds of α-Si_3N_4 powders with different properties (high purity and low purity) were pressureless sintered using $MgAl_2O_4$-ZrO_2 as sintering additives. The grain growth was controlled by sintering time and temperature. The fracture toughness was determined using indentation microfracture (IM) and single-edge-precracked-beam (SEPB) methods. A discrepancy of fracture toughness was found between the values obtained by these two methods, and the SEPB method provided higher fracture toughness than the IM method. Materials with more large elongated Si_3N_4 grains gave higher fracture toughness, R-curve behavior and larger discrepancy. This is contributed to the effects of grain bridging, pull-out and deflection by the large elongated Si_3N_4 grains. Comparing the specimens from two kinds of α-Si_3N_4 powders with different purity level, both gave high fracture toughness of over 9 MPa $\cdot$ $m^{1/2}$ by the SEPB method, while the E10 samples have a little higher flexural strength.

1. Introduction

Dense silicon nitride (Si_3N_4) ceramics is a promising material in many engineering applications primarily due to its high strength, especially high toughness, as compared to other structural ceramics [1–3]. The high toughness was caused from the rode-like β grain morphology which improve the fracture toughness by crack bridging [4] and deflection [5] toughening mechanisms. The rode-like β grain is formed by an abnormal grain growth of β-Si_3N_4 grains during sintering [6], and then the fracture toughness of Si_3N_4 ceramics can reach to as high as 8 to 11 MPa$\cdot m^{1/2}$.

In the evaluation of the fracture toughness, various testing methods such as single-edge-precracked-beam (SEPB), single-edge-notched-beam (SENB), Chevron-notched-beam (CN), indentation microfracture (IM) measurement, indentation strength beam (ISB), and double torsion (DT) are used for ceramic materials. The most widely and favorably used methods are the SEPB and the IM methods, because the SEPB method has a sharp crack tip representing the actual stress intensity situation, and the IM method is very simple and requires much smaller specimen size than any other tests. Study shows that there is no unique fracture toughness value for the Si_3N_4 with the R-curve behavior [7], suggesting that there should be a discrepancy in fracture toughness values measured by different methods. The Si_3N_4 materials with the rod-like grain structure tend to present the higher toughness and large discrepancy.

Because the SEPB and IM methods are often used to determine the fracture toughness of ceramics, it should be explicit that which microstructural factors affect this discrepancy and how large it is. In the present study, Si_3N_4 ceramics were fabricated by pressureless sintering, and the grain growth of Si_3N_4 was controlled by changing the sintering temperature and time. The IM and SEPB methods were used to determine the fracture toughness. The effect of β-Si_3N_4 grain growth on the fracture toughness and its discrepancy were investigated. The relationship among grain growth, fracture toughness and measurement methods will be discussed.

2. Experimental

Two commercially available α-Si_3N_4 powders with fairly different characteristics: high purity Si_3N_4 from the imide method (SN-E10, UBE Industries, Tokyo, Japan) and low purity Si_3N_4 from the direct nitridation of Si (SN-9S, Denka corp., Tokyo, Japan) were used as the matrix materials in this investigation. $MgAl_2O_4$ and ZrO_2 (MA-Z) were used as sintering additives. Some properties of the Si_3N_4 powders used and compositions of testing materials were shown in Tables I and II respectively. The mixture was wet milled in ethanol for 24 h, then dry milled for another 4 h and finally passed through a 500 μm sieve. The resultant powders were uniaxially pressed at a pressure of 30 MPa before being cold isostatically pressed at 200 MPa. The sintering

* Author to whom all correspondence should be addressed. *Present Address:* Superplastic Nano-science Laboratory, Material Structural Formation Process Department. National Industrial Research Institute of Nagoya, 1-1 Hirate-Cho, Kita-Ku, Nagoya, 462-8510, Japan.

TABLE I Some properties of Si_3N_4 powders used in the present work

Property	α-Si_3N_4 from the imide method (SN-E10)	α-Si_3N_4 from the Si direct nitridation (SN-9S)
α-phase content (%)	97	92
Average grain size (μm)	0.55	1.10
Specific surface area (m^2/g)	11	7.3
Impurity: Cl (ppm)	<50	
Fe (ppm)	<50	1200
Al (ppm)	<50	1200
Ca (ppm)	<10	1200

TABLE II Composition of testing materials

Material	Sample	Si_3N_4 powder	$MgAl_2O_4$ (wt %)	ZrO_2 (wt %)
9S-MA-Z	SSN-1	9S	1.0	1.0
	SSN-2		2.5	2.5
	SSN-3		5.0	5.0
	SSN-4		7.5	7.5
	SSN-5		10.0	10.0
E10-MA-Z	ESN-1	E10	2.5	2.5
	ESN-2		5.0	5.0
	ESN-3		7.5	7.5

was hold at 1850 and 1900 °C with a nitrogen pressure of 0.6 MPa. The keeping time at 1850 °C was 4 and 12 h, and that at 1900 °C was 8 h to obtain the different grain morphology.

The samples were machined to bending test bars with a size 40 × 4 × 3 mm (JIS R1601). The tensile surface was ground and polished with 9 μm, 2 μm diamond pastes and finally ultrafine Al_2O_3 paste. Densities were measured by the Archimede's method. The edges on the tensile surface were beveled to reduce the effect of edge cracks. Three-point bend testing (span of 30 mm) was used to determine the flexural strength using a testing machine (Autograph AG-10TC, Shimadzu Co. Ltd., Kyoto, Japan) under a cross-head displacement speed of 0.5 mm/min.

Fracture toughness was determined by two methods: indentation microfracture measurement (IM) and single-edge-precracked-beam (SEPB). In the IM method, indentation were made with a Vickers diamond pyramid on the polished surface of bending bars by Vickers hardness tester (AVK-C2, Akashi Co. Ltd., Tokyo, Japan). Five loads (P) of 50, 100, 200, 300 and 500 N were used. Hardness was calculated from diagonal of the indentation and contact load. Fracture toughness was calculated from measurement of the crack profile length (C) using the equation given by Niihara [8]. Six indents were made at each indentation load. In the SEPB method [9], samples with an acceptable crack configuration specified by JIS1607 were used to determine fracture toughness. The precracked specimens were tested at a stroke rate of 0.01 mm/min using three points bending fixture with a span of 16 mm using the same testing machine as the bending strength test. The fracture toughness was calculated by the formula given by JIS1607. Six specimens were used to determine the average value of the fracture toughness.

The specimens for scanning electron microscopy (SEM) observation were prepared by plasma etching and chemical etching with NaOH at 350 °C for 2 min. The microstructure of the sintered body was observed using the SEM (Model S-5000, Hitachi, Japan). The grains were traced on the transparent paper on the SEM micrographs. More than 500 grains were measured statistically for each sample by an image analysis software (National Institute of Health (NIH) Image 1.57). SEM was also used to investigate fracture surfaces and crack propagation paths.

3. Results and discussion

SEM microstructures are shown in Fig. 1 for Si_3N_4 ceramics sintered at 1900 °C/8 h with different sintering

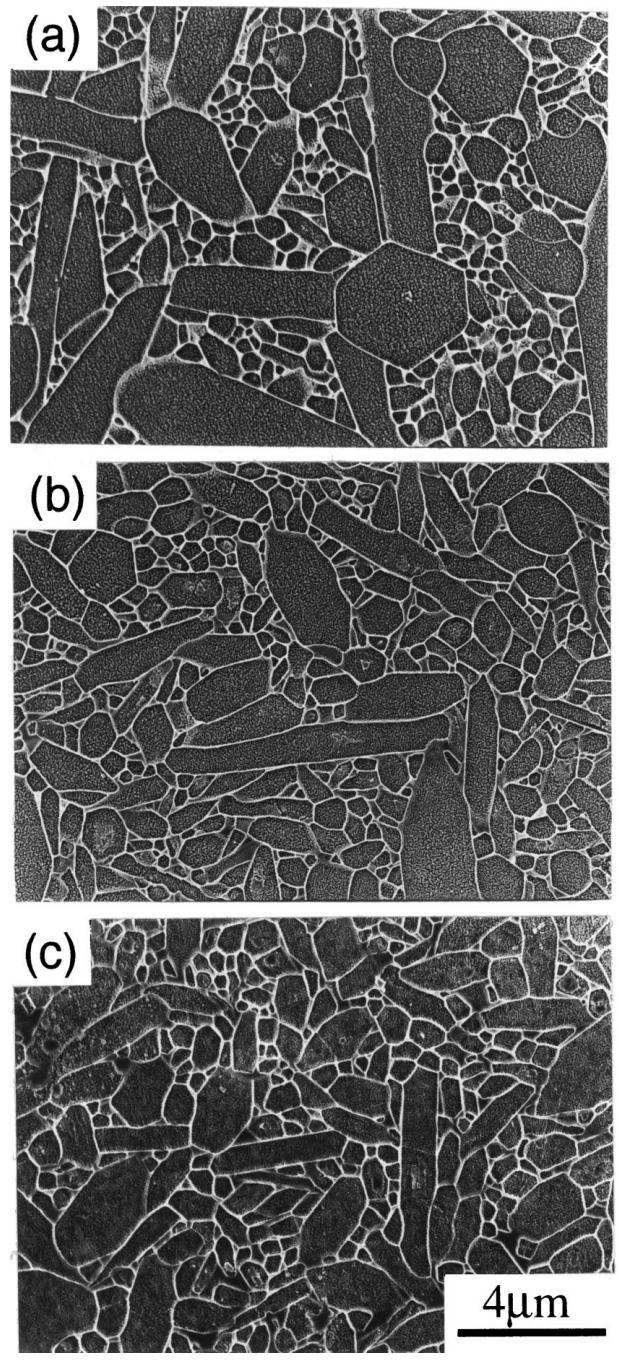

Figure 1 SEM microstructures of Si_3N_4 with different sintering additive content: (a) ESN-1, (b) ESN-2, (c) ESN-3. Sintering condition: 1900 °C/8 h.

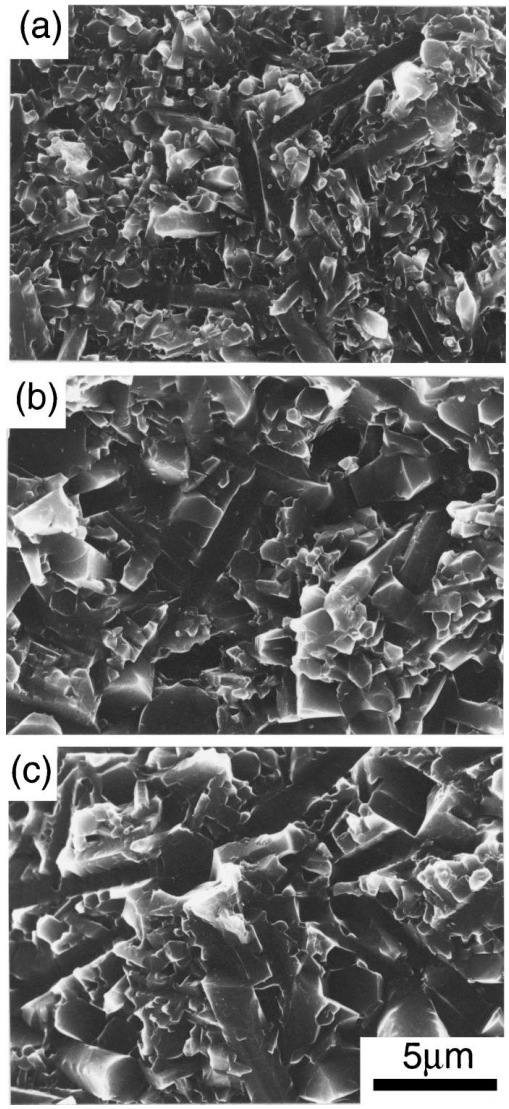

Figure 2 SEM microstructures the fracture surface of ESN-1 specimen obtained at different sintering conditions. (a) 1850 °C/4 h, (b) 1850 °C/12 h, (c) 1900 °C/8 h.

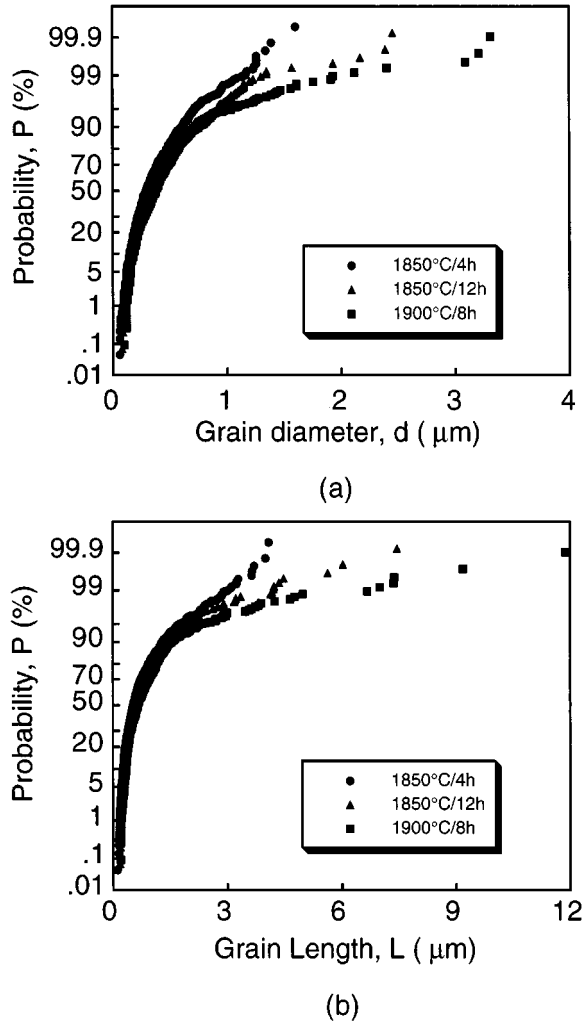

Figure 3 Grain size distribution of ESN-1 specimen obtained by different sintering conditions. (a) grain diameter, (b) grain length.

additive content. It is clear that the material with a small content of additives has a bimodal microstructure, i.e., coarse elongated grains within a fine grain matrix. The material with large content of additives is composed of mainly fine grains. The number of coarse elongated β-grains apparently decreases with the increase of the content of the sintering additives, indicating that the growth of Si_3N_4 grains is inhibited by the sintering additives. Fig. 2 shows SEM micrographs of fracture surfaces for the ESN-1 samples made with the three sintering conditions. It is clear that the large grains are developed with increasing sintering time and temperature.

Image analysis of the grains was carried out to quantitatively evaluate the microstructure. Fig. 3 shows the grain diameter (d) and grain length (L) distribution. From the figure, it can be seen that the specimen sintered at the condition of 1900 °C/8 h shows relatively more large elongated grains. Usually to the two-dimension image of Si_3N_4, the coarse grains are small in number, but represent a significant fraction of the total area measured [10]. Considering that contribution of fine matrix grains to the fracture resistance is minor compared to that of the coarse elongated grains, characteristics of large grain were determined and analyzed, where the large grain defined as $d > 3d_{ave}$ [11]. For these large grains, average diameter, length and aspect ratio, number and area fraction were determined and shown in Table III. The specimen obtained at 1900 °C/8 h showed the largest size and highest fraction of large grain in number and area, and that at 1850 °C/4 h showed the lowest. The results suggest that formation and growth of the large grain was affected by the sintering temperature and time as shown in Fig. 2.

Studies pointed out that some coarse elongated grains having a high aspect ratio were developed in the matrix with finer and equiaxed grains when the Si_3N_4 powders were fired at 1800 to 2000 °C by way of a gas-pressure sintering technique [6, 12]. Mitomo [13] studied the grain growth of β-Si_3N_4 and found that the number and

TABLE III Average length, diameter, aspect ratio, number and area fraction of large grains ($d > 3d_{ave}$) for different sintering conditions

Sintering condition	Length (μm)	Diameter (μm)	Aspect ratio	Number fraction (%)	Area fraction (%)
1850 °C/4 h	2.53	1.23	2.05	0.75	13.66
1850 °C/12 h	3.76	1.81	2.01	1.15	17.01
1900 °C/8 h	4.23	1.93	2.14	3.10	44.99

area fraction of large grain had no relationship with sintering temperature, which was determined by the number and size of large grains in starting powders. For the sintering of α-Si_3N_4 powder, however, grain nucleation and growth of β-Si_3N_4 occurred during the sintering, which were affected by the sintering temperature and time. A small additive content was preferable for developing the coarse elongated grain [11]. Solution-reprecipitation process was the main mechanism for grain growth of Si_3N_4 [14], in which diffusion through liquid phase occurs at grain boundaries. β-Si_3N_4 grain growth is rate controlled by diffusion through the liquid phase and occurs to a significant extent by coalescence [15]. A fast diffusion velocity promotes the grain growth of Si_3N_4 resulting in more large grains in number and area fraction. Obviously high sintering temperature and long sintering time result in coarse grain morphology. As shown in Fig. 1, the samples with small additive content had a relative coarse grain morphology. This is come from the fact that small additive content provides a thin liquid phase between Si_3N_4 grain and the diffusion velocity is promoted.

Fig. 4 shows the fracture toughness obtained by the IM method for the Si_3N_4 ceramics from different sintering condition. Loads from 50 to 500 N were used to determine the relationship between fracture toughness and indentation load. From the figure it can be seen that samples obtained at the sintering conditions of 1900 °C/8 h and 1850 °C/12 h present relatively higher toughness than that at 1850 °C/4 h. An increase of fracture toughness with indentation load was observed for the samples obtained at former two sintering conditions, while the samples at 1850 °C/4 h did not show such increase. The increase of fracture toughness with the indentation load indicates a fracture resistance (*R*-curve) behavior that the fracture toughness increases with increasing crack length. The *R*-curve behavior is often happened for the materials with large elongated Si_3N_4 grain morphology [16] due to its effect on the grain bridging, pull-out and deflection. As a result, the discrepancy of toughness at the different indentation load is generally observed because of the fracture resistance.

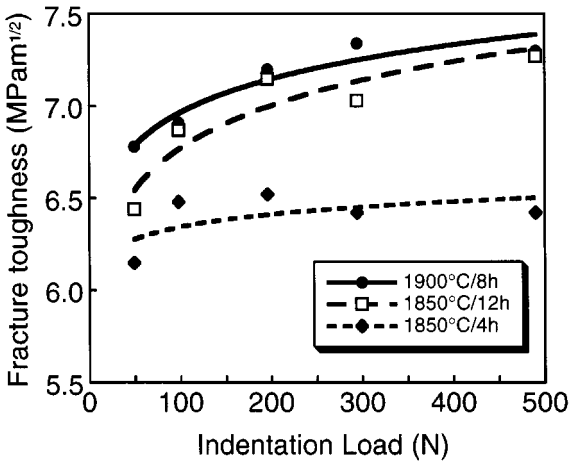

Figure 4 Fracture toughness of the materials fabricated by different sintering condition as a function of the indentation loads. The material with large grain matrix shows increased toughness with the load (*R*-curve).

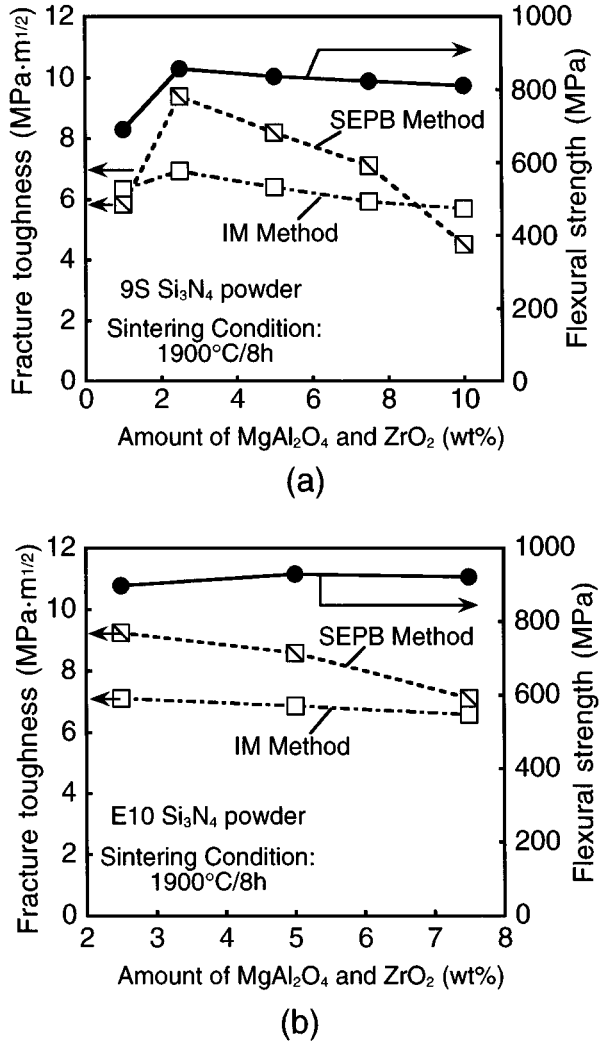

Figure 5 Fracture toughness and corresponding strength versus sintering additive content for (a) 9S-MA-Z, (b) E10-MA-Z.

Fig. 5 shows the fracture toughness and corresponding flexural strength as a function of the sintering additive content for the specimens sintered at 1900 °C/8 h. The fracture toughness at the indentation load of 200 N by the IM method was used to compare with that by the SEPB method. The toughness and strength are shown for material made by two kinds of starting powder and different amount of sintering additives. The E10 samples show the strength of ∼900 MPa, while the 9S samples show a little lower strength of 800–850 MPa. From these figures it can be seen that the materials with a small amount of sintering additives showed the relatively higher toughness and larger discrepancy than those with a large one. The SSN-1 is an exception because of the low densification caused by the lower additive content. Fig. 6 shows the comparison of fracture toughness by the IM and SEPB methods for three different sintering conditions. The material with low sintering additive content (total 5 wt %) within each kind were tested as the low sintering additive content promote the grain growth and fracture toughness. From the figure it is clear that the discrepancy is smallest for the material sintered at 1850 °C/4 h, while at 1900 °C/8 h that is largest. The samples from two kinds of row powder also show almost the same discrepancy in fracture toughness.

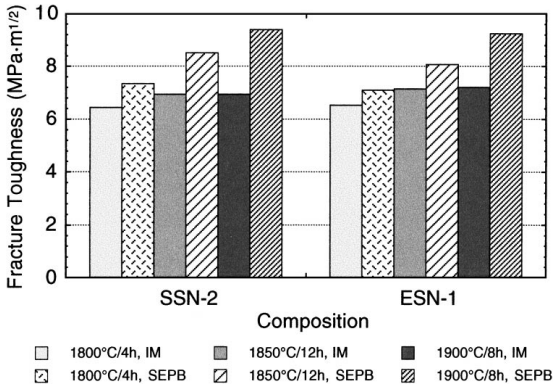

Figure 6 Fracture toughness and corresponding strength versus sintering condition for three different ceramics containing small amount of sintering additives.

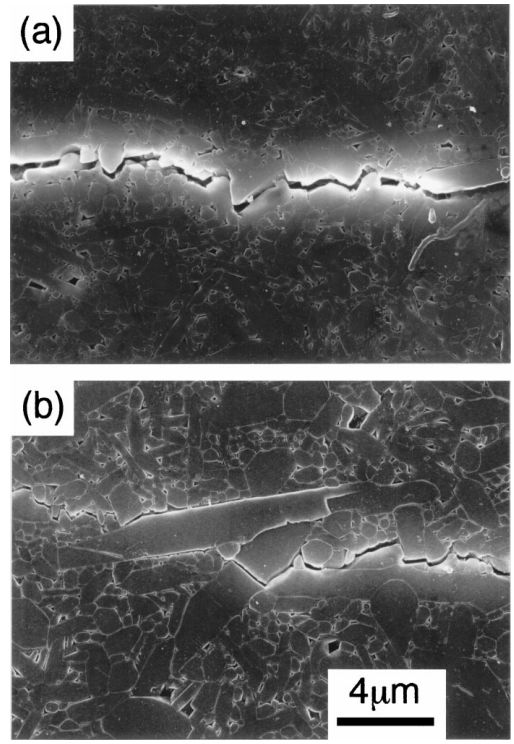

Figure 7 Scanning electron micrographs of crack propagation of Si_3N_4 (ESN-1) sintered at (a) 1850 °C/4 h, (b) 1900 °C/8 h.

The large discrepancy in fracture toughness obtained by the different testing methods was also reported in other papers. Choi [7] measured the fracture toughness of one Si_3N_4 material with four kinds of test methods. He obtained the fracture toughness 5.76 MPa·m$^{1/2}$ by IM and 10.16 MPa·m$^{1/2}$ by SEPB and explained this discrepancy from the effect of rising *R*-curve behavior of materials. Because the *R*-curve is obtained with only indentation strength test, it can not represent the actual situation of SEPB or CN methods. The elongated grains in silicon nitride have been well documented to result in the improved long-crack toughness [17, 18]. The large and elongated grains enhance the crack bridging, pull-out and deflection that give a rising *R*-curve. Thus a long crack toughness may induce the discrepancy between fracture toughness values by different measurements. The rising *R*-curve behavior and discrepancy are basically caused by the existence of the large elongated grains.

The crack behavior confirmed the mechanism of increasing fracture toughness and discrepancy of toughness value in sintered specimens. Polished surface were indented using a pyramid Vickers indenter, followed by the chemical etching. The propagating crack paths were investigated to analyze the toughening mechanisms. It is reported that the toughening mechanism is changed concerning to the diameter of elongated grains [19]. For thin needle grains with diameters of <1 μm, elastic bridging and pull-out were observed, whereas for thick needle grains of >1 μm frictional bridging and deflection were shown. Fig. 7 shows typical crack paths of specimens with different grain morphology which was obtained at two sintering conditions as 1850 °C/4 h and 1900 °C/8 h. The crack trajectory shows that the crack in the specimen made at 1850 °C/4 h propagates through the equiaxed microstructure having little bridging and deflection and along a relatively straight line. For the specimens fabricated at 1900 °C/8 h, the crack passes through the boundaries of fine grains as well as the coarse grains oriented at low angles, resulting in the crack bridging and deflection by the coarse elongated Si_3N_4 grains resulted a tortuous crack path. The difference of crack morphology between these two specimens is caused by the difference in large elongated Si_3N_4 grain. As obviously the large elongated grain resulted in the increase in fracture toughness, it was also considered as a main reason to induce the large discrepancy of fracture toughness. This can be explained by the fact that the grain bridging or deflection and pull-out absorb the fracture energy. Comparing with the IM method, the SEPB method provides a long propagating crack front where the high possibility of grain bridging and pull-out exists. Thus corresponding with the enhancement of the fracture toughness, a discrepancy between the different measurements was also happened simultaneously.

In the present work two raw Si_3N_4 powders were used to compare their effect on the microstructure and mechanical properties. Although the low purity Si_3N_4 powder (9S) is much cheaper than high-purity Si_3N_4 powder (E10), the fracture toughness levels and the discrepancy of 9S ceramics reached to almost same as E10 ceramics, while the strength of the 9S ceramics (800–850 MPa) is a little lower than that of E10 ceramics ($\sim$900 MPa). Measured by the IM method, the fracture toughness of E10 samples was a little higher, but by the SEPB method that of the 9S samples was a little higher (Fig. 6). Under the sintering condition of 1900 °C/8 h, ESN-1 and SSN-2 obtained a high fracture toughness of $\sim$7 MPa·m$^{1/2}$ by IM and $\sim$9.5 MPa · m$^{1/2}$ by SEPB. The lead to conclude that the impurity of Si_3N_4 powder has no influence on the fracture toughness and its discrepancy between the values obtained by different test methods.

4. Conclusion

The influence of grain growth of Si_3N_4 on the fracture toughness and its discrepancy caused by different test methods was studied using two kinds of raw powders.

High value and large discrepancy of fracture toughness between IM and SEPB methods were found to occur in the Si_3N_4 materials with large elongated grain morphology. This is due to the effect of grain bridging, deflection and pull-out of the elongated grains. Thus, the high fracture toughness is always accompanied by the large discrepancy for the materials with the large elongated grains. The impurity of Si_3N_4 has no influence on the fracture toughness and discrepancy. Special care should be paid when the fracture toughness will be measured for the Si_3N_4 with the large elongated grain. On addition, the following observation should be noted: The samples with low amount of sintering additives showed the high fracture toughness and low purity Si_3N_4 powder (9S) is competitive with the high purity Si_3N_44 powder (E10) in some application fields.

References

1. E. TANI, S. UMEBAYASHI, K. KISHI, K. KOBAYASHI and M. NISHIJIMA, *Amer. Ceram. Soc. Bull.* **65** (1986) 1311.
2. K. H. JACK, *J. Mater. Sci.* **11** (1976) 1135.
3. G. ZIEGLER, J. HEINRICH and G. W TTING, *J. Mater. Sci.* **22** (1987) 3041.
4. P. F. BECHER, C. H. HSUEH, P. ANGELINI and T. N. TIEGS, *J. Amer. Ceram. Soc.* **71** (1988) 1050.
5. K. T. FABER and A. G. EVANS, *Acta Metall.* **31** (1983) 565.
6. M. MITOMO and K. MIZUNO, *Yogyo-Kyokaishi* **94** (1986) 106.
7. S. R. CHOI and J. A. SALEM, *J. Amer. Ceram. Soc.* **77** (1994) 1042.
8. K. NIIHARA, R. MORENA and D. P. H. HASSELMAN, *ibid.* **65** (1982) C-116.
9. T. NOSE and T. FUJII, *ibid.* **71** (1988) 328.
10. H. L. O'DONNELL, M. J. READEY and D. KOVAR, *ibid.* **78** (1995) 849.
11. Y. W. KIM, M. MITOMO and N. HIROSAKI, *J. Mater. Sci.* **30** (1995) 4043.
12. M. MITOMO and S. UENOSONO, *J. Amer. Ceram. Soc.* **75** (1992) 103.
13. M. MITOMO, M. TSUTSUMI, H. TANAKA, S. UENOSONO and F. SAITO, *ibid.* **73** (1990) 2241.
14. M. MITOMO and S. UENOSONO, *J. Mater. Sci.* **26** (1991) 3940.
15. H. BJÖRKLUND, L. K. L. FALK, K. RUNDGREN and J. WASÉN, *J. of the Eur. Ceram. Soc.* **17** (1997) 1285.
16. C. W. LI, D. J. LEE and S. C. LUI, *J. Amer. Ceram. Soc.* **75** (1992) 1777.
17. C. W. LI and J. YAMANIS, *Ceram. Eng. Sci. Proc.* **10** (1989) 632.
18. C. W. LI, S. C. LUI and J. GOLDACKER, *J. Amer. Ceram. Soc.* **78** (1995) 449.
19. P. SAJGALIK, J. DUSZA and M. J. HOFFMANN, *ibid.* **78** (1995) 2619.

Received 23 July 1998
and accepted 6 May 1999